Original Article

Alfacalcidol as A Protective Agent Against Gastrocnemius Muscle Damage after Atorvastatin Intake: A Histological and Biochemical Study

Zainab M Altaib[1], Doaa M Khaled[1, 2], Mohamed S Mohamed[1]

Department of Histology and Cytology, Faculty of Medicine, [1]Helwan University, [2]MUST University, Cairo, Egypt

ABSTRACT

Background and Objective: Atorvastatin (Ator) is widely used to lower blood cholesterol but often causes muscle-related side effects. Alfacalcidol (Alf), a vitamin D analog, has shown positive effects on muscle health. This study aimed to elucidate the possible protective role of Alf on gastrocnemius muscle damage after Ator intake in male albino rats.

Materials and Methods: Thirty-six adult male albino rats were randomly divided into three groups: Group I (Control; n = 12), Group II (Ator-treated; n = 12), and Group III (Ator and Alf-treated; n = 12). Group II received Ator (10 mg/kg/day) in 0.5 ml distilled water containing 2 mg Ator. Group III received Alf (1 µg/kg/day) concomitantly with Ator, prepared by crushing and dissolving tablets in 0.5 ml distilled water. All drugs were administered orally for 4 weeks. Twenty-four hours after the last dose, rats were sacrificed under anesthesia by intraperitoneal injection of phenobarbital (80 mg/kg). A biochemical study for creatine phosphokinase (CPK) was performed. Muscle specimens were dissected and examined using light microscopy (Hematoxylin and Eosin, Masson's trichrome, and PAS stains) and electron microscopy. Morphometric and statistical analyses were conducted.

Results: Group II showed histological changes indicating myopathy and degenerative changes, which regressed in Group III. The mean CPK values significantly increased in Group II compared to the control and Group III.

Conclusions: Alfacalcidol demonstrated a definitive protective effect against Ator-induced skeletal muscle damage, confirmed through biochemical and histological analyses. Alf can be recommended for hypercholesterolemic patients on Statins, particularly those at risk of vitamin D deficiency.

Key Words: Alfacalcidol, muscle damage, special stains, statin, ultrastructure.

Revised: 19 October 2024, **Accepted:** 20 November 2024

Corresponding Author: *Doaa Mabrouk Khaled*, MD, *Department of Histology and Cytology, Faculty of Medicine, Helwan University, Cairo, Egypt,* **Tel.:** *+201149939631*, **E-mail:** *doaa.khaled@med.helwan.edu.eg.*

ISSN: 1110-0559, June 2024, Vol. 8, No. 1.

INTRODUCTION

Statins are among the most prescribed medications worldwide. They are extensively used to lower the risk of heart attacks, strokes and other cardiovascular problems, as well as to reduce mortality from these conditions[1]. The primary use of Statins is to manage high cholesterol levels. They work by inhibiting the enzyme 3-hydroxy-3-methylglutaryl-coenzyme A (HMG-CoA) reductase, which is crucial in the body's cholesterol production process[2].

A study has shown that Statins reduce the risk of acute respiratory distress syndrome and fetal complications in patients with COVID-19[3]. These effects may be due to the diverse actions of Statins. Recent research suggests that Statins might directly inhibit the entry and replication of SARS-CoV-2 in cells. They may also work through indirect mechanisms unrelated to coronavirus infection, such as reducing inflammation, preventing blood clots or enhancing blood function[4].

Statins are either fat-soluble (like Simvastatin and Atorvastatin) or water-soluble (like Pravastatin and Rosuvastatin). Water-soluble Statins are mainly absorbed by liver cells through specific transporters, resulting in high liver concentrations but limited distribution elsewhere. Fat-soluble Statins, however, can spread throughout the body and are absorbed by liver cells via passive diffusion[5].

Atorvastatin, a member of the Statin family, has many side effects that can interfere with its use. It has been reported to affect the liver, kidneys and muscles. The most frequent side effect of Statin therapy and the main cause of Statin withdrawal, is Statin-associated myalgia[6].

The way Statins cause muscle damage and muscle-related side effects isn't fully understood. Researchers have suggested several possible explanations, such as the depletion of important metabolic products or the triggering of programmed cell death[7]. A case of drug-related myonecrosis following long-term use

 DOI: 10.21608/jmh.2024.329545.1133

of Atorvastatin was reported, monitored by serum markers such as CPK[8].

Alfacalcidol is an active metabolite of vitamin D and plays an important role in regulating the contraction, proliferation and differentiation of skeletal muscle fibers. It has been proven that vitamin D affects muscle tissue through both direct and indirect mechanisms[9].

Alfacalcidol is regarded as one of the steroidal agonists of the vitamin D receptor (VDR). Its maximum specificity for binding to muscle VDR is due to its OH group in the 1α position. Multiple studies have found that vitamin D influences muscle performance when its active form, $1,25(OH)_2D$, attaches to specific receptors, promoting muscle development. A comprehensive review of research indicates that taking vitamin D supplements can decrease muscle problems associated with Statin use. Additionally, low levels of 25(OH)D in the body have been connected to muscle-related side effects from Statins[11]. It has been proven that Statin side effects on the musculoskeletal system may be minimized by vitamin D restoration and coenzyme Q supplementation[12].

The aim of the current study was to evaluate the possible protective effect of Alf on gastrocnemius muscle damage after intake of Ator in male albino rats, expressed by histological changes and confirmed by biochemical and morphometric studies.

MATERIALS AND METHODS

Experimental design and animals:

The study was conducted at the animal house of the Faculty of Veterinary Medicine, Banha University, following local approval. The duration of the study was 4 weeks. It involved 36 adult male albino rats, aged 3 months and weighing between 200 - 250 grams. The rats were kept in a controlled environment with a 12-hour light/dark cycle and a temperature maintained at 22 ± 2°C. They were housed in groups of no more than 4 rats per cage, with standard-sized cages providing adequate space for normal social behavior. The environment had appropriate humidity and ventilation and the rats had unrestricted access to food (grains) and water. All experimental procedures adhered to ethical guidelines and were approved by the Research Ethics Committee of the Faculty of Medicine at Helwan University (approval number 22 - 2020).

The medications were freshly prepared each day and administered orally via a gastric tube. This dosing regimen began on the first day of the experiment and continued until 24 hours before the animals were anesthetized. The rats were randomly divided into three equal groups, each containing 12 rats.

Group I (Control group): all rats received 0.5 ml of distilled water daily.

Group II (Ator-treated): Each rat received Ator (10 mg/kg/day). A daily dose of 0.5 ml of distilled water containing 2 mg of Ator was administered to each rat[7].

Group III (Ator and Alf-treated): Each rat received Ator as in group II and Alf (0.5 µg/kg/day). Additionally, each rat was given 0.5 ml of distilled water daily, containing 0.1 µg of Alf[13].

Reagents:

Atorvastatin (Ator): "The medication, marketed under the brand name ATOR by the Egyptian International Pharmaceutical Industries Company, was available in 20 mg tablet form. These tablets were ground into a powder and dissolved in distilled water.

Alfacalcidol (Alf): Trade name (BON-ONE), Minipharm Egypt, in the form of tablets (each 1 µg active ingredient). It is prepared by crushing and dissolving it in distilled water.

Blood samples and biochemical study:

"Before anesthetizing the rats, blood samples were collected from their tail veins using heparinized capillary tubes. These samples were analyzed for creatine phosphokinase (CPK) at the Biochemistry Department of Banha University's Faculty of Medicine. CPK is an enzyme that indicates muscle damage and is commonly measured in blood tests to diagnose conditions such as myositis and rhabdomyolysis[14].

Histological Studies:

Twenty-four hours after the last dose, the rats were sacrificed following anesthesia via intraperitoneal injection of phenobarbital (80 mg/kg)[15]. Specimens from the gastrocnemius muscle were dissected and excised. These specimens were then processed for examination under electron and light microscopes.

a. Electron microscopic (EM)examination:

Small pieces of the gastrocnemius muscle, about 1 mm in size, were extracted. These samples were initially treated with 3 % glutaraldehyde for 3 hours. They were then further processed using 1 % osmium tetroxide in a 0.1 M phosphate buffer solution (pH 7.4) at 4°C for 2 hours. The samples underwent dehydration and were embedded in resin to form solid blocks. Using a diamond knife, extremely thin sections (50 - 80 nm thick) were cut from these blocks and placed on copper grids. These sections were stained first with a saturated uranyl acetate solution in 50 % ethanol, followed by lead citrate. Finally, the prepared samples were examined using a Transmission EM (TEM, specifically the JEOL 100 OX model)[16].

b. Light microscopic (LM) examination:

Additional tissue samples underwent a series of preparatory steps: they were first preserved in a 10 % formaldehyde solution, then rinsed with tap water. Following this, the samples were progressively dehydrated using increasing concentrations of alcohol. Next, they were cleared using xylene. The samples were then successively immersed in soft paraffin for 45 minutes and hard paraffin for another 45 minutes. Finally, they were embedded in hard paraffin and arranged into blocks. Paraffin sections of 5 - 6 micrometer thickness were cut and subjected for:

1. Hematoxylin and Eosin (H and E) staining[17].
2. Masson's trichrome stain (M.T) for demonstration of collagen fibers[17].
3. PAS stain for demonstration of glycogen substance[18].

Morphometric study:

Image analysis was conducted using a Leica Qwin 500 C image analyzer computer system, manufactured by Leica Imaging System LTD (England). This analysis took place at the Central Research Lab of Tanta University, Faculty of Medicine. For each slide in both the control and experimental groups, ten different areas were chosen at random, ensuring they didn't overlap. These areas were examined at 400x magnification to perform the assessment.

a- Area % of degenerated muscle fibers.

b- Area % of collagen fibers.

c- The optical density of glycogen content.

Statistical Study:

Statistical study was done using the statistical package of social science (SPSS) version 25 (SPSS Inc., USA). The results were presented as averages with their corresponding standard deviations. Statistical analysis was performed using Analysis of Variance (ANOVA) followed by post hoc tests. Any p-value equal to or less than 0.05 was considered statistically significant[19].

RESULTS

Biochemical results:

The mean plasma level of CPK enzyme of group II (Ator-treated) showed a significant increase when compared with that of group I (control) ($P \leq 0.05$), While group III (Ator and Alf treated) showed a non-significant increase when compared with that of group I (control) ($P > 0.05$) and showed significant decrease when compared with that of group II (Ator-treated) ($P \leq 0.05$) (Table 1), (Histogram 1: Figure 1).

Table 1: Mean values (± SD) of serum CPK level in control and experimental groups:

Experimental Groups	Mean Plasma level of CPK enzyme ± SD (IU/L)
Group I (control)	122.76 ± 9.03
Group II (Ator treated)	314.65 ± 40.59*
Group III (Ator and Alf treated)	143.50 ± 24.77 $

SD: Standard Deviation.

Significant results at $P \leq 0.05$.

* Significant increase versus group I and III.

$ Significant decrease versus group II.

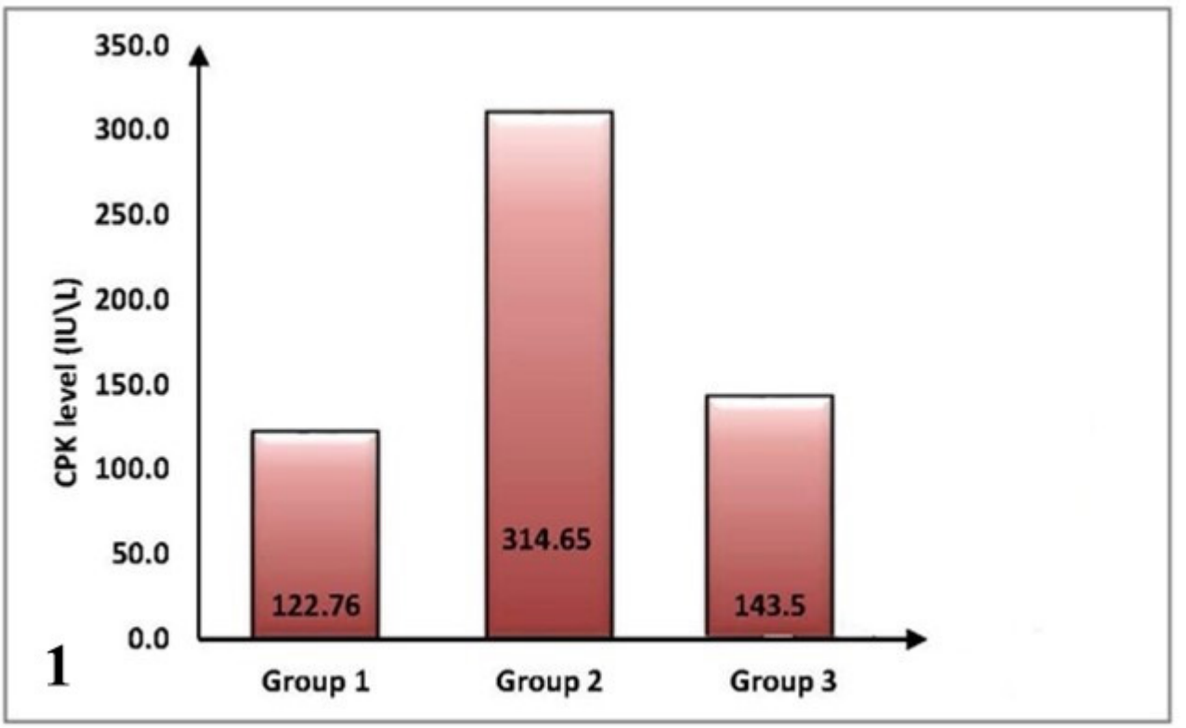

Figure 1 (Histogram 1): The mean plasma level of CPK enzyme of all groups.

Histological Results

1. Hematoxylin and Eosin (H and E) results:

In group I (Control), longitudinal sections (L.S) of the skeletal muscle fibers appeared cylindrical, parallel and of uniform thickness with multiple peripheral oval nuclei. Fibers are separated by connective tissue (C.T) endomysium. The sarcoplasm appeared acidophilic and crossly striated (Figure 2a). In transverse sections (T.S), the muscle fibers appeared polygonal with peripheral oval nuclei. The individual muscle fibers are separated by C.T. endomysium (Figure 2b). Group II (Ator treated), L.S revealed disorganized, fragmented and discontinued muscle fibers with variability in size and shape and some of them showed darkly stained nuclei. In addition, the sarcoplasm appeared either deeply acidophilic in focal areas of muscle fibers or lightly stained in others. The endomysium and perimysium appear edematous with some vacuoles, mononuclear cell infiltration and congested blood capillaries are seen (Figure 3a).

Other fields of group II showed variations in size and shape of muscle fibers with distortion of its normal architecture as many fibers acquired irregular outline rather than polygonal with widening of endomysium and perimysium with deposition of fat. Some muscle fibers show lysis and dissolution and others show tapering of ends. Some fibers exhibit darkly stained nuclei while others exhibit rounded pale centrally located nuclei (Figure 3b). Group III (Ator and Alf treated) demonstrated minimal disintegration and disarrangement of few muscle fibers otherwise most fibers are parallel cylindrical with acidophilic cytoplasm and multiple peripheral nuclei. Few of muscle fibers have central nuclei with nearly normal endomysium (Figure 4).

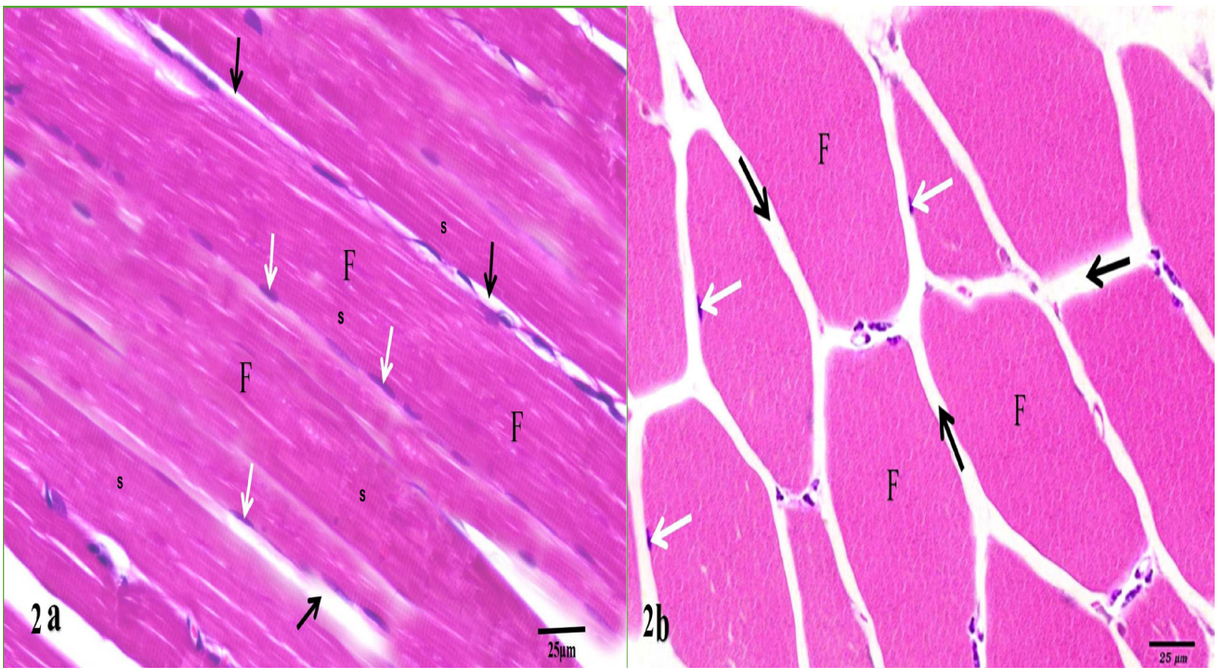

Figure 2: H and E stained sections of rat gastrocnemius muscle of group I (control): (a): L.S shows cylindrical parallel muscle fibers (F) of uniform thickness and acidophilic sarcoplasm with clear transverse striations (s). Multiple peripheral oval nuclei were seen (white arrows). The muscle fibers are separated by C.T endomysium (black arrows). (b): T.S shows polygonal skeletal muscle fibers (F) and peripheral oval nuclei (white arrows). Muscle fibers are separated by C.T endomysium (black arrows). (a,b x400).

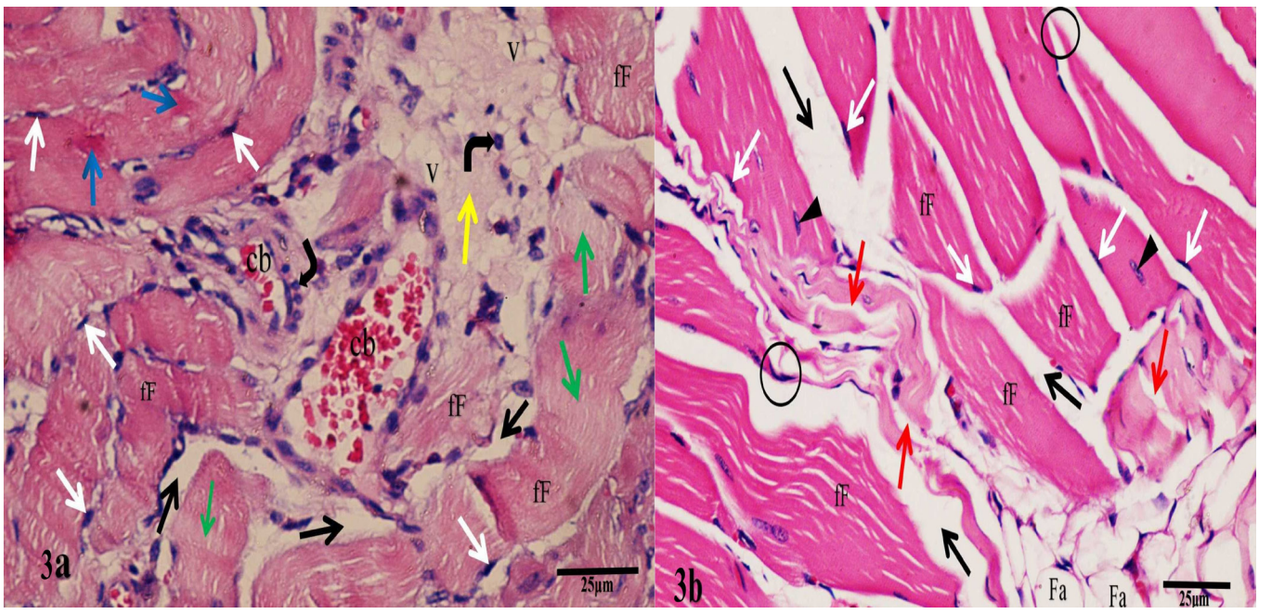

Figure 3: H and E stained sections of rat gastrocnemius muscle of group II (Ator treated): (a): L.S shows disorganized, fragmented and discontinued muscle fibers (fF) with irregularity in size and shape and darkly stained nuclei (white arrows). Areas of hyper-eosinophilic sarcoplasm (blue arrows) are demonstrated. Other fibers show focal areas of lightly stained sarcoplasm (green arrows). The endomysium (black arrows) and perimysium (yellow arrow) appeared oedematous with some vacuoles (V) and mononuclear cells infiltration (curved black arrows). Congested blood capillaries (cb) are seen in the perimysium. (b): T.S shows many fragmented muscle fibers (fF) with irregular outlines rather than polygonal. Lysis and dissolution of some fibers (red arrows), others have tapering ends (black circles). Some fibers exhibit darkly stained nuclei (white arrows), others exhibit rounded pale centrally located nuclei (black arrow heads). The endomysium (black arrows) appears wide and the perimysium shows fat deposition (Fa). (a,b x400).

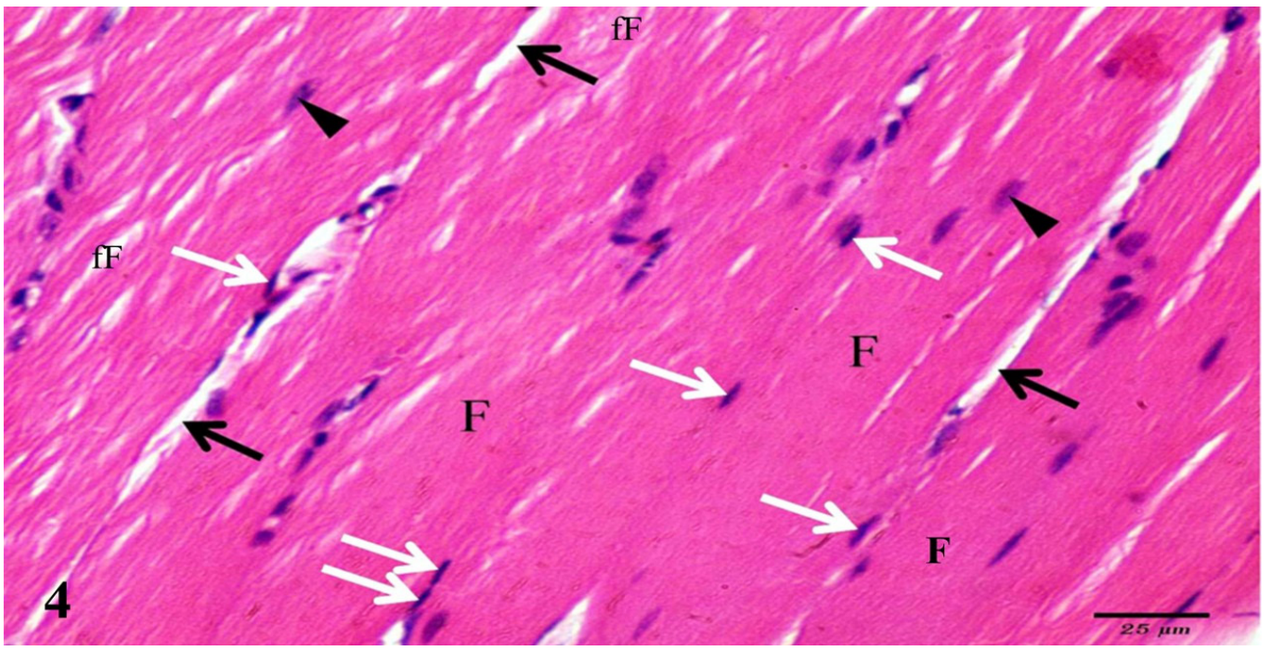

Figure 4: H and E stained L.S of rat gastrocnemius muscle of group III (Ator and Alf treated) exhibits parallel and cylindrical fibers (F). Few fibers still show minimal disintegration and disarrangement (fF). The sarcoplasm appears acidophilic with multiple peripheral oval nuclei (white arrows). Few muscle fibers have central slightly pale nuclei (black arrow heads). Nearly normal endomysium (black arrows). (x400)

2. Masson's trichrome results:

Group I showed a minimal presence of collagen fibers in the endomysium (Figure 5a). In contrast, Group II exhibited an extensive accumulation of collagen fibers in both the endomysium and perimysium (Figure 5b). In group III, a mild amount of collagen fibers was observed in the endomysium (Figure 5c).

3. Periodic acid Schiff (PAS) results:

In Group I, two distinct types of muscle fibers were observed. Some fibers displayed a strong PAS-positive reaction (stars), while others exhibited a weak reaction (thin arrows) (Figure 6a). Group II demonstrated a significant reduction in PAS-positive content (Figure 6b), while Group III showed a notable recovery of PAS-positive content (Figure 6c).

Electron microscope results:

In **group I (Control)**, gastrocnemius muscle from this group displayed typical normal ultrastructural features. The myofibrils were found to be organized in a uniform pattern, aligned parallel to the muscle fiber's longitudinal axis. These myofibrils exhibited the characteristic striated appearance, with alternating light (I) and dark (A) bands clearly visible. An oval-shaped nucleus was observed positioned beneath the sarcolemma. Within this nucleus, the heterochromatin was distributed along the inner surface of the nuclear envelope and a nucleolus was also discernible (Figure 7a). A pale, narrow H band was observed cutting across the A band, with a distinct dark M-line running through the center of the H band. The Z-line was visible dividing the light band in half and sarcomeres were located between two consecutive Z-lines (Figure 7b). Additionally, mitochondria and sarcoplasmic reticulum cisternae appeared under the sarcolemma. There are also glycogen granules between myofibrils and under the sarcolemma (Figure 7c).

Group II (Ator treated) showed degeneration of some of myofibrils and disruption of the characteristic patten of dark and light bands. The nucleus has irregular shape and boundaries with fragmented discontinued chromatin which mildly condensed. The sarcoplasm is densely packed with mitochondria of varying sizes and shapes, with some showing damaged cristae. Additionally, the cisternae of the sarcoplasmic reticulum appear swollen and an abundance of connective tissue fibers is also observed (Figure 8a). Disruption of Z line and affected I band with obviously dilated sarcoplasmic reticulum cisternae are observed (Figure 8b).

Group III (Ator and Alf treated) showed parallel myofibrils that were like the control group, consisting of dark A bands, light I bands and dark Z lines. There were minor areas with Z line disarrangement. A nucleus with condensed chromatin was located at the periphery. Some mitochondria appeared in between the myofibrils and the sarcoplasmic reticulum cisternae were apparently intact (Figure 9).

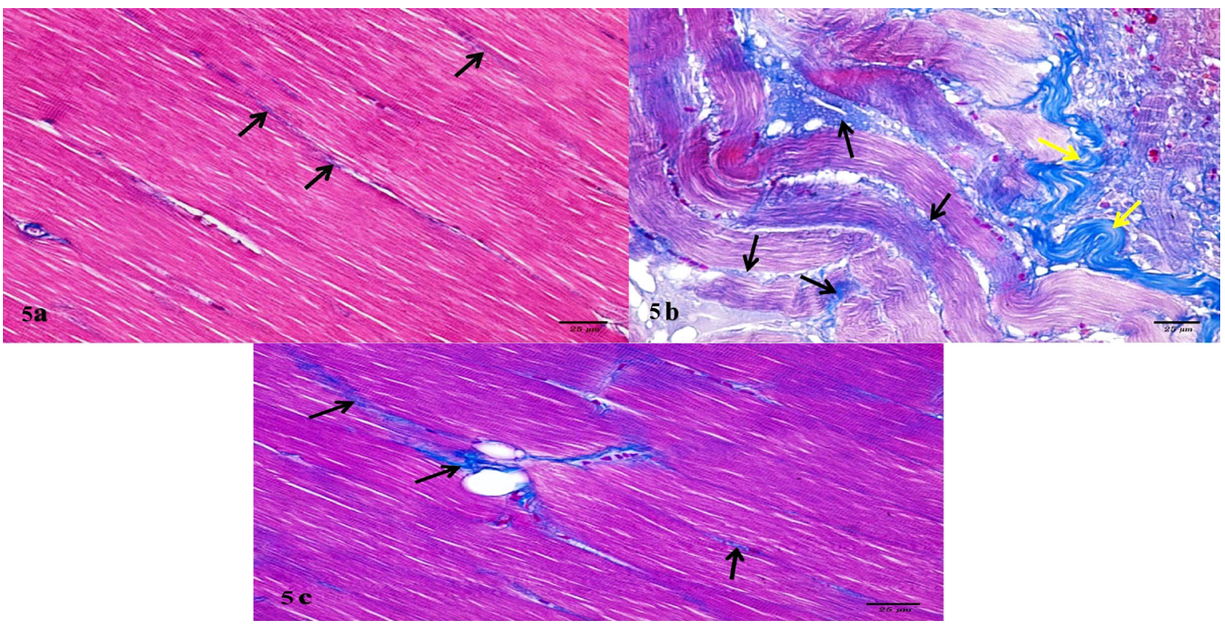

Figure 5: Masson's trichrome stained L.S of rat gastrocnemius muscle: (a): group I (control) shows minimal collagen fibers (black arrows) in endomysium. (b): group II shows extensive deposition of collagen fibers (black arrows) in the endomysium and perimysium (yellow arrows). (c): group III shows mild deposition of collagen fibers (black arrows) in the endomysium. (a, b, c x400).

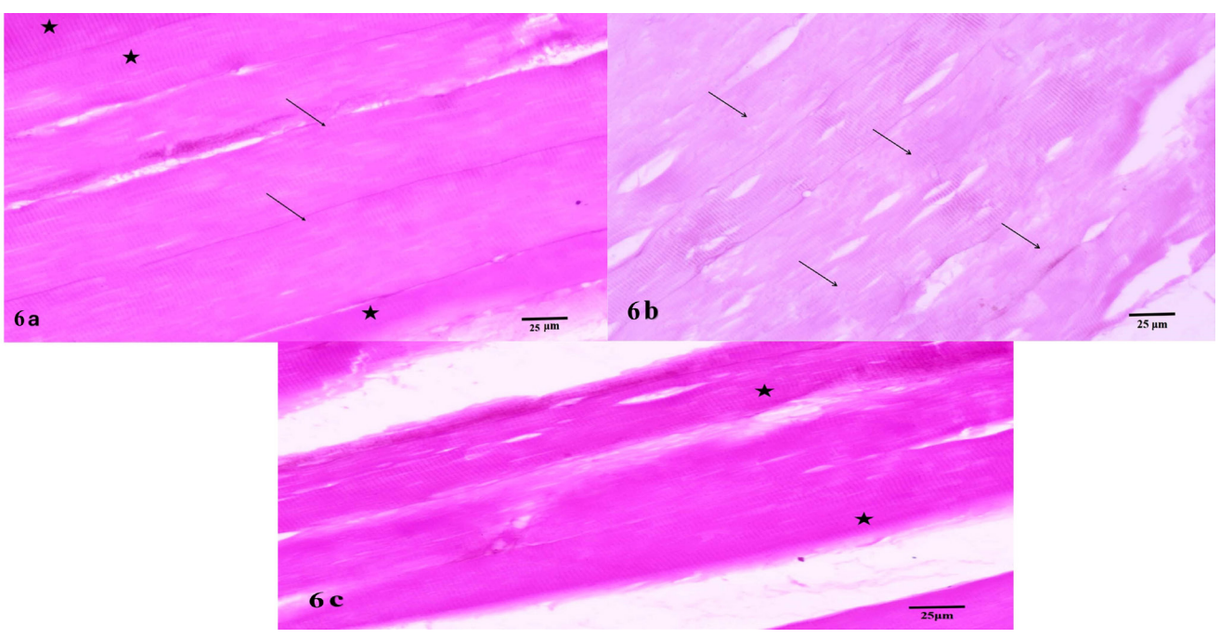

Figure 6: PAS-stained L.S of rat gastrocnemius muscle (a): group I shows two types of muscle fibers. Some fibers showed intense PAS +ve reaction (stars) while others had faint reaction (thin arrows). (b): group II shows a marked decrease in PAS +ve contents (thin arrows). (c): group III shows marked restoration of PAS +ve contents (stars). (a, b, c x400).

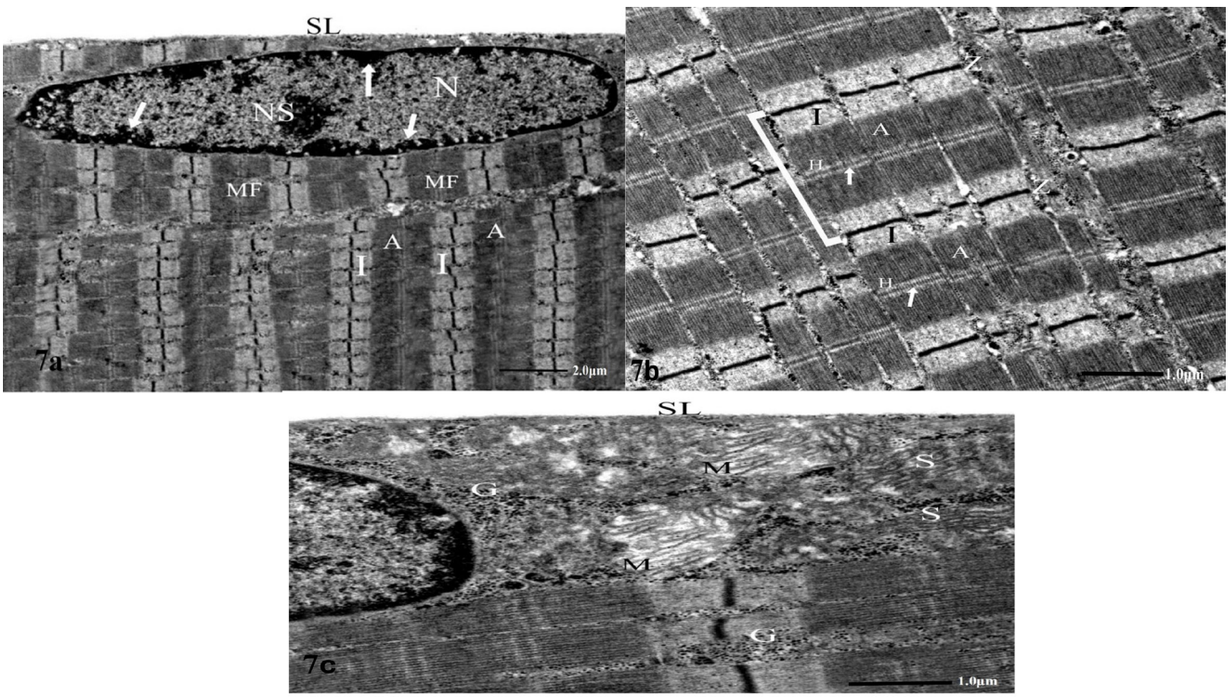

Figure 7: EM sections of rat gastrocnemius muscle of the group I (Control): (a) Parallel arrangement of myofibrils (MF) with alternating light (I) and dark (A) bands. Oval elongated euchromatic nucleus (N) with prominent nucleolus (NS) and parts of peripheral heterochromatin (arrows). The nucleus lies just beneath the sarcolemma (SL). (TEM X 2500). (b): Parallel arrangement of myofibrils with alternating light (I) and dark (A) bands. A pale narrow region, the H band (H), was seen transecting the A band with a dark M-line (white arrows) in the middle of the H band. Sarcomeres ([ ) are seen between two successive Z lines (Z). (TEM X 5000). (c): The mitochondria (M) beneath the sarcolemma (SL). Notice the presence of sarcoplasmic reticulum cisternae (S (and glycogen granules (G). (TEM X 8000).

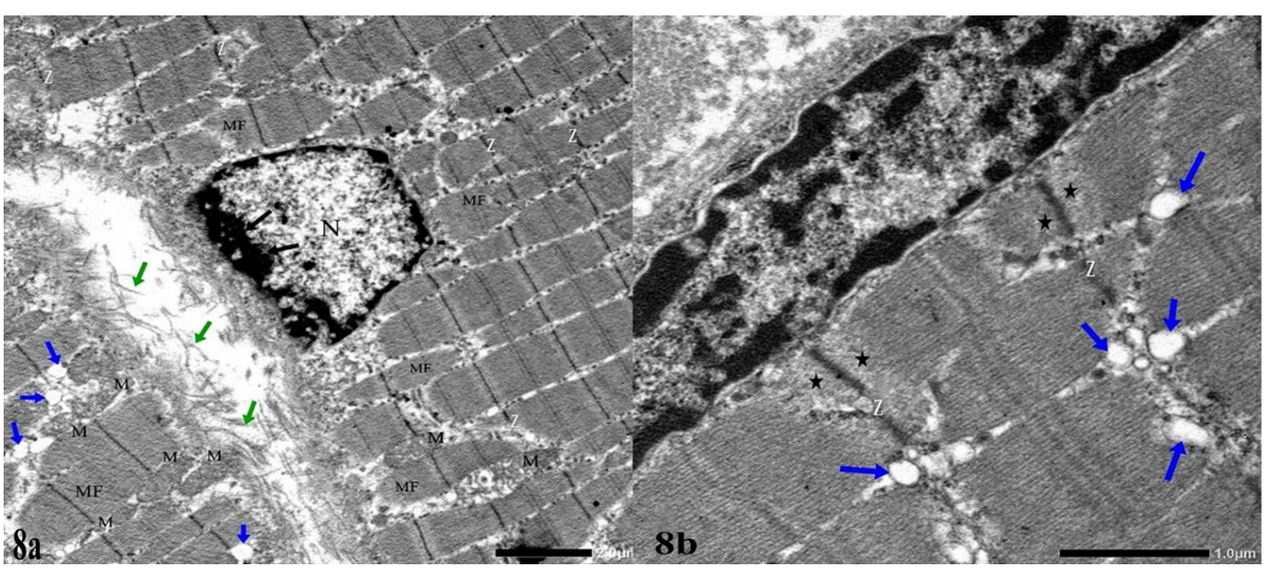

Figure 8: EM sections of rat gastrocnemius muscle of group II (Ator treated): (a) Degenerated myofibrils (MF) and disruption of its striations. Disruption of Z lines are noticed (Z). Abnormal irregular nucleus (N) with mild condensation of its chromatin (black arrows). Intermyofibrillar mitochondria (M) are variable in size and shape, some of them with destructed cristae. Mild dilatation of sarcoplasmic reticulum cisternae (blue arrows). Excess C.T fibers (green arrows) in the endomysium around the sarcolemma. (TEM X 2500). (b): EM section of rat gastrocnemius muscle of group II shows obviously disruption of Z line (Z) and affected I band (stars). Obviously dilated sarcoplasmic reticulum cisternae (blue arrows). (TEM: X 8000).

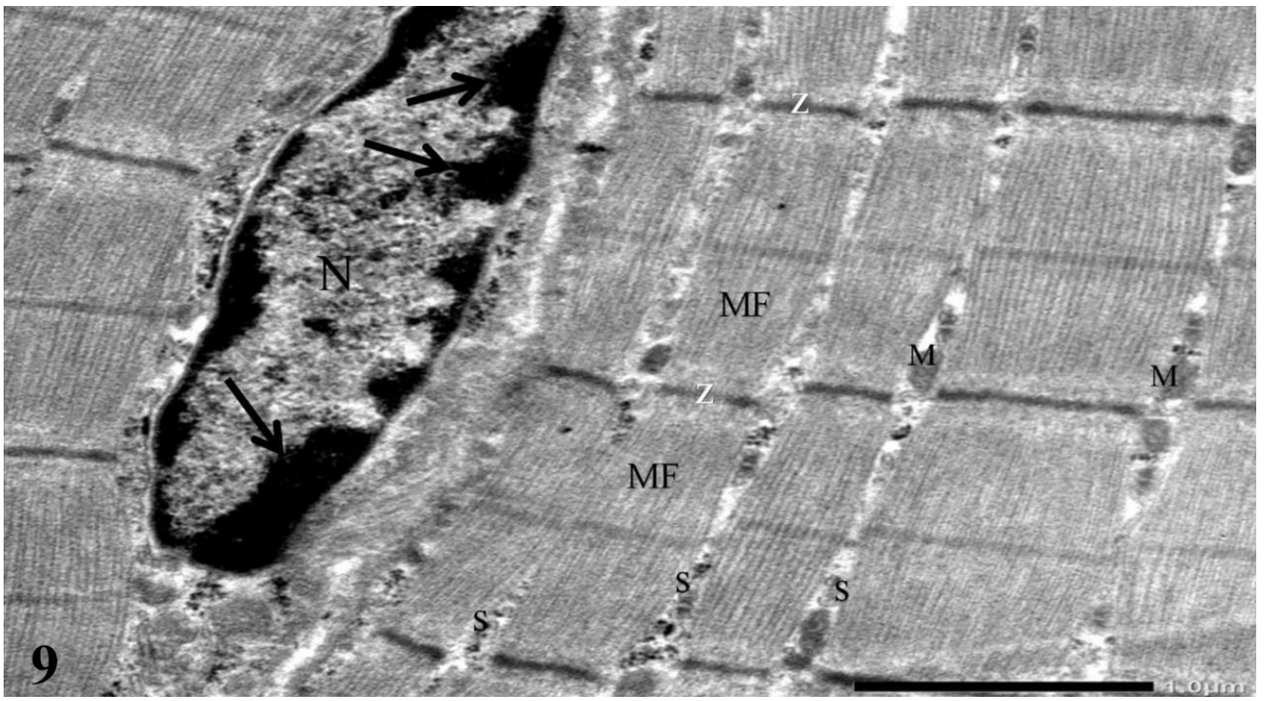

Figure 9: EM section of rat gastrocnemius muscle of group III shows apparently normal parallel myofibrils (MF) with mild disarrangement of Z line (Z). Some mitochondria appear in between the myofibrils (M). Apparently normal sarcoplasmic reticulum cisternae (S). A peripheral nucleus (N) with condensed chromatin (black arrows) is clearly seen around the nuclear envelope. (TEM X 8000).

Morphometric results:

1. Mean area % of degenerated muscle fibers:

The mean area percentage of degenerated muscle fibers (characterized by fragmentation, discontinuity, irregular size and shape and darkly stained nuclei) in group II showed a significant increase compared to the control group ($P \leq 0.05$). In contrast, group III exhibited a non-significant increase compared to group I (control) ($P > 0.05$) and a significant decrease compared to group II ($P \leq 0.05$) (Table 2), (Histogram 2: Figure 10).

Table 2: The mean values (± SD) of area % of degenerated muscle fibers in control and experimental groups:

Groups	Area % of degenerated muscle fibers
Group I (control)	13.62 ± 0.16
Group II (Ator treated)	52.18 ± 0.25*
Group III (Ator and Alf treated)	21.5 ± 0.68 $

SD: Standard Deviation.

Significant results at $P \leq 0.05$.

* Significant increase versus group I and III.

$ Significant decrease versus group II.

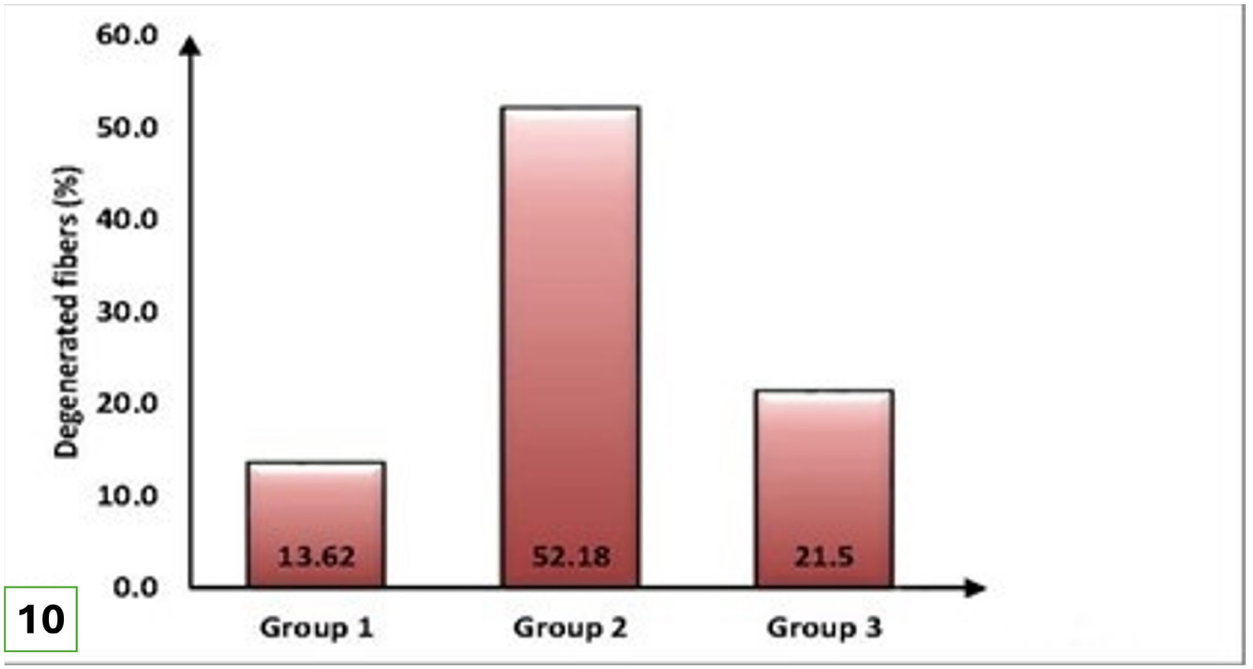

Figure 10 (Histogram 2): The mean values (± SD) of area % of degenerated muscle fibers in all experimental groups.

2. Mean area % of collagen fibers:

The mean area of collagen fibers in group II showed a significant increase compared to the control group ($P \leq 0.05$). Group III demonstrated a non-significant increase compared to the control group (Table 3), (Histogram 3: Figure 11).

Table 3: The mean area % of collagen fibers ± SD in all experimental groups:

Groups	The mean area % of collagen fibers (Mean ± SD)
Group I (control)	7.31 ± 0.46
Group II (Ator treated)	38.14* ± 0.81
Group III (Ator and Alf treated)	13.69∞ ± 0.53

SD: Standard Deviation.

Significant results at $P \leq 0.05$.

* Significant increase versus group I and III.

∞ Non-significant increases versus group I.

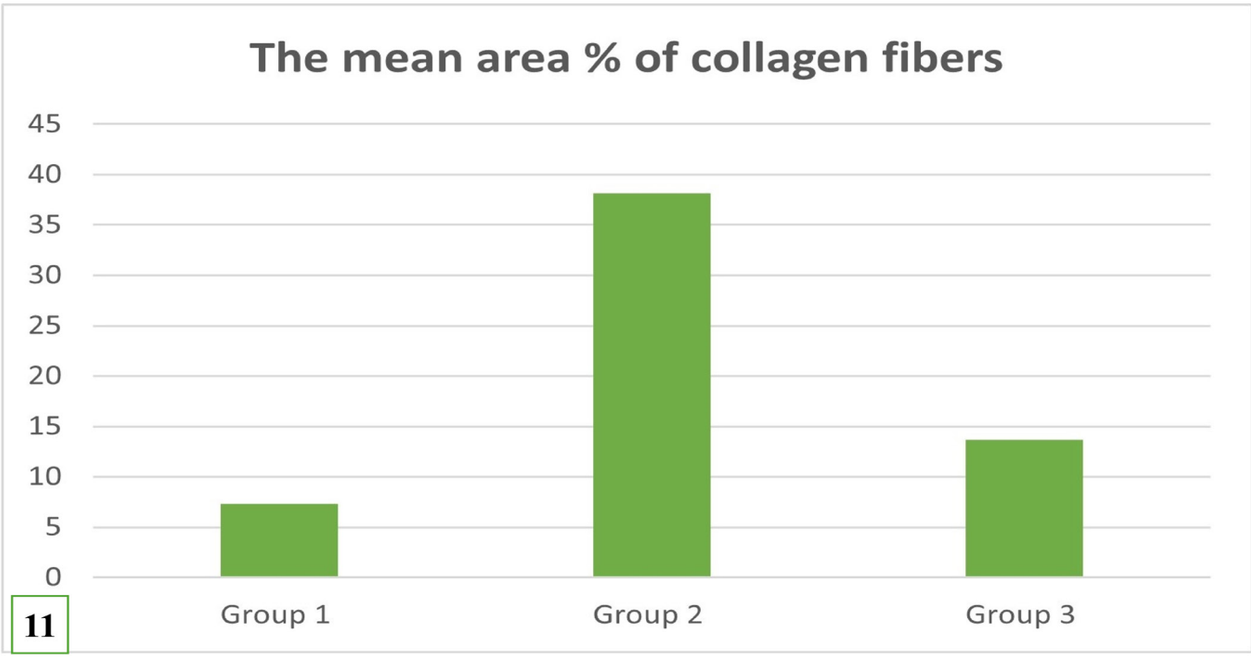

Figure 11 (Histogram 3): The mean area % of collagen fibers ± SD in all experimental groups.

3. Optical density measurements of the PAS staining intensities:

The mean area of PAS staining intensities in group II showed a significant increase compared to the control group ($P \leq 0.05$). However, in group III, a non-significant increase was recorded compared to the control group (Table 4), (Histogram 4: Figure 12).

Table 4: The optical density measurements of the PAS staining intensities ± SD in all experimental groups:

Groups	The mean of optical density (Mean ± SD)
Group I (control)	0.86 ± 0.04
GroupII (Ator treated)	0.19* ± 09-1.08
Group III (Ator and Alf treated)	0.65∞ ± 0.04

SD: Standard Deviation.

Significant results at $P \leq 0.05$.

* Significant increase versus group I and III.

∞ Non-significant increases versus group I.

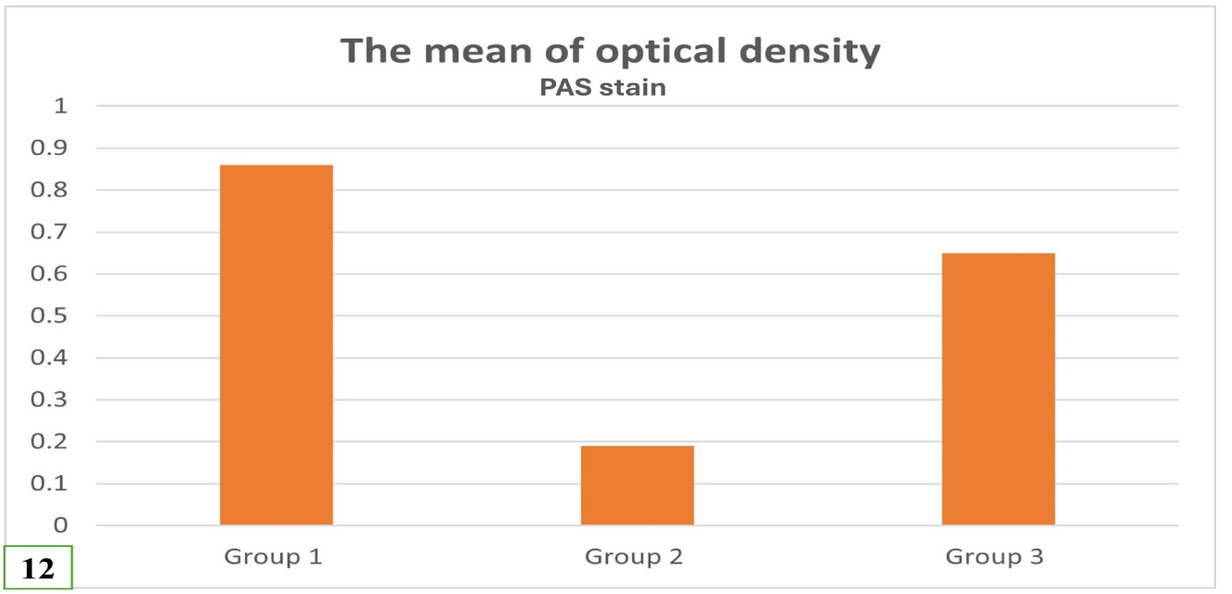

Figure 12 (Histogram 4): The optical density measurements of the PAS staining intensities ± SD in all experimental groups.

DISCUSSION

Statins have dramatically transformed the treatment of cardiovascular conditions[1]. The enzyme HMG-CoA reductase plays a key role in the pathway for cholesterol synthesis. Statins work by inhibiting this enzyme, leading to a reduction in the production of low-density lipoprotein cholesterol (LDL-C)[2]. Additionally, Statins may have positive effects on other lipid levels, potentially increasing high-density lipoprotein cholesterol (HDL-C) and affecting triglyceride levels. They can also reduce vascular inflammation and enhance endothelial cell function[20].

Statins' side effects can lead to decreased patient compliance. These effects include myalgia, myopathy, rhabdomyolysis, liver toxicity and gastrointestinal problems[6]. Patients who do not achieve desired cholesterol levels with lower doses often need higher doses, which increases their risk of developing myopathy[21].

Creatine phosphokinase (CPK) is a marker in myopathic processes[22]. Creatine phosphokinase levels are used to monitor the safety of Statin use. The author added that the Statin treatment should be immediately stopped if CPK levels exceed ten times the upper limit of normal.

Group II in the present study exhibited a significantly higher mean plasma CPK level compared to both Groups I and III. In contrast, Group III showed a non-significant elevation relative to the control group, but a significant reduction compared to Group II. Decreased CPK levels can compromise muscle structure, as CPK plays a crucial role in maintaining the tight lattice in the sarcomeres' M-region, thus influencing the stability of contracting filaments. This finding aligns with the study conducted by[23].

Biochemically, elevated CPK levels may reflect the histological evidence of myopathy observed in the gastrocnemius muscle. This muscle was chosen for study because it predominantly consists of type II white fibers[24]. Type II fibers are known to be more susceptible to Statin-induced myopathy compared to type I fibers. While Statins at low doses primarily affect type II fibers, higher doses can impact type I fibers as well[7]. Furthermore, Reduced gene expression of peroxisome proliferator-activated receptor gamma coactivator-1α (PGC-1α) expression provides an additional reason for the pale, glycolytic muscle fibers' heightened vulnerability to muscle injury[25].

By LM examination, Group II (Ator-treated) sections revealed disorganized, fragmented and discontinued muscle fibers with variability in size and shape. Some of them showed darkly stained nuclei. Similarly, degenerated and disorganized muscle fibers were found in the skeletal muscle of

rats treated with Atorvastatin and vitamin D"[26]. The observed variation in fiber sizes in this group was explained by atrophy and compensatory hypertrophy in some fibers. Muscle atrophy could result from either an elevated rate of protein breakdown, reduced protein synthesis or a combination of these processes[26]. Statin therapy was found to inhibit the HMG-CoA reductase pathway, leading to disrupted protein synthesis and resulting in muscle fiber atrophy. Moreover, Statins activate skeletal ryanodine receptors (RyR1), which could be a critical factor in the onset of myopathy[27].

The sarcoplasm appeared either deeply acidophilic in focal areas of muscle fibers or lightly stained in others. These findings indicate cytoplasmic protein denaturation. The endomysium appeared edematous and contained vacuoles, fat deposition, mononuclear cell infiltration and congested blood capillaries. It was reported that the infiltration of mononuclear cells in the endomysium and perimysium likely results from the release of particular mediators during myocyte degeneration, leading to an inflammatory reaction and the recruitment of inflammatory cells[28].

Other fields show lysis and dissolution of some muscle fibers and tapering ends of others. This might be related to destroyed mitochondria and myofilament loss[29]. Other fibers exhibit darkly stained nuclei and others exhibit rounded pale nuclei that are centrally located. These findings confirm the incidence of skeletal muscle fiber inflammation that progressed to degeneration. This is consistent with new studies showing that muscle injury activates satellite cells, causing them to multiply. These activated cells, termed myoblasts, can form myotubules with centrally located vesicular nuclei[30].

Our results of Masson trichrome staining confirm significant collagen fiber deposition in the endomysium and perimysium. A recent study observed numerous collagen fibers within these areas in Masson and Van Gieson-stained muscle sections[31]. A progressive increase in collagen fibers was noted, correlating with the extent of muscle damage. It has been observed that an increase in intrafascicular connective tissue typically indicates a response to myofiber loss, where fibroblasts replace damaged areas and form collagen fibers[24]. An alternative explanation, supported by other researchers, suggests that this fibrotic process is promoted by the release of growth factors like platelet-derived growth factor and transforming growth factor-β1, which trigger myogenic cell differentiation into myofibroblasts and stimulate extracellular matrix cells to produce collagen[32].

In the current study, PAS staining also confirmed glycogen storage disorder in Group II which revealed a marked decline in PAS contents. In contrast, group III recruited a marked restoration of PAS contents. These results align with those of Hedberg-Oldfors *et al.,* 2019[33]. Morphometric and statistical analyses confirmed the previous findings, revealing a sig rise in the mean area percentage of degenerated muscle fibers and collagen fiber deposition in Group II compared to the control and Group III. Furthermore, Group II exhibited a sig decrease in PAS content compared to the other groups.

Electron microscopy examination of group II in this study showed degeneration of certain myofibrils and disruption of the normal dark and light band pattern, including the Z line. The nucleus exhibited an irregular shape with fragmented and somewhat condensed chromatin. The sarcoplasm was packed with mitochondria of different sizes and shapes, some with damaged cristae and the sarcoplasmic reticulum cisternae were notably dilated. These results are consistent with those reported by[22], who proposed that disfigured mitochondria in the Ator-treated group might help maintain ATP production during apoptosis caused by reactive oxygen species.

Moreover, a lack of prenylated protein, another substance that is important to the HMG-CoA reductase pathway, causes odd intracellular signaling, myofiber vacuolation, organelle enlargement and ultimately apoptosis. This theory could account for the appearance of sarcoplasmic reticulum's dilated cisternae[34]. The mitochondrial dysfunction observed may help clarify the previously described issues. Furthermore, it has been reported that Statins can alter membrane properties by inhibiting the production of ubiquinone, which impairs mitochondrial ATP synthesis. This disruption in the energy metabolism of myocytes can result in plasma membrane damage, pyknosis, vacuolation of the myofibers and swelling of organelles[34].

It has been documented that Statins increase cytosolic calcium which activates caspase-3 and leads to cell death and apoptosis[35]. This could account for the presence of darkly stained nuclei observed within certain muscle fibers in the present study. An alternative theory posits that Statins may affect mitochondrial function by impairing the respiratory chain, which reduces ATP levels and boosts ROS production. This process can cause mitochondrial membrane permeability transition, cytochrome c release into the cytosol and subsequent apoptosis. Concurrently, Statins are linked to mitochondrial

dysfunction and disturbances in the Akt/mTOR signaling pathway, leading to enhanced protein degradation in skeletal muscle, reduced protein synthesis and activation of apoptosis[36].

Evidence indicates that Ator impairs mitochondrial activity and oxygen usage by diminishing the ubiquinone content in muscle fibers, which subsequently enhances lactate production[37]. This metabolic abnormality could prompt the accumulation of lipids within myocytes and consequently causes of myopathy[38].

The degenerative changes observed under LM and EM were linked to the cumulative effects of Statins on the sarcolemma, disrupting the muscle fibers' ion transport system and initiating degeneration. Statins damage muscle cells by altering membrane cholesterol content, with muscle cells being particularly vulnerable due to their unique lipid and protein distribution[26]. The authors explained that reduced cholesterol levels affect membrane fluidity and impair sodium-potassium pump function, potentially leading to organelle degeneration and cell damage. These mechanisms explain the observed structural alterations in muscle tissue at the microscopic level, highlighting the complex interplay between Statins, cellular membranes and muscle fiber integrity.

Alfacalcidol, 1α- hydroxyl vitamin D3, is a synthetic vitamin D analog that regulates calcium and is frequently used to treat osteoporosis. Vitamin D has been shown to have an anabolic effect on muscular tissue, as it promoting the synthesis of muscle cytoskeletal protein[39]. It is considered one of the steroidal VDR agonists. It exhibits the highest specificity for binding to VDR in muscle[22]. Notably, for patients with high cholesterol who experience muscle pain and weakness from Statin use, vitamin D supplementation often enables them to resume Statin treatment without these adverse effects[40].

Our choice was to utilize Alf (1α-(OH) D3 as it has a decreased risk of hypercalcemia and hypercalciuria, because following oral administration and intestinal absorption, it must be activated in the liver via 25-hydroxylation. Hence, in contrast to calcitriol, it exhibits a slower plasma concentration curve[41]. Additionally, Alf activation is unaffected by liver disease, except in cases of advanced cirrhosis.

In the current study, serum CPK levels were significantly lower in group III (Ator and Alf treated) compared to group II (Ator treated) and did not differ significantly from the control group. This could account for the histological improvement observed in the LM results, which showed minimal disintegration of muscle fibers. The muscle fibers appeared as parallel cylindrical fibers with acidophilic cytoplasm, multiple peripheral nuclei, a few central nuclei and apparently normal endomysium. These findings were confirmed by Masson trichrome and PAS-stained sections, which revealed a mild amount of collagen fibers in the endomysium and perimysium and strong PAS content compared to group II. These results are in line with other studies[31, 33]. The previous findings indicated a clear amelioration of the degenerative changes that developed in group II.

By ultrastructural examination of group III, parallel myofibrils arranged almost similarly to those of the control group are observed. However, certain areas show myofibrillar dissolution and lysis. Other areas exhibit disarrangement of myofibrils and Z lines. A peripherally located nucleus with mildly condensed chromatin is seen. Intermyofibrillar mitochondria are either normal or have fragmented cristae, with seemingly normal sarcoplasmic reticulum cisternae. These findings are consistent with records of Chogtu *et al.*, 2020[26].

Morphometrically, the improvements in degenerated muscle fibers achieved by Alf in group III might be explained by the theory that skeletal muscle vitamin D receptors regulate different transcription factors in muscle cells, encouraging the growth of muscle cells and their differentiation into mature type II muscle fibers[42]. An additional rationale for the observed enhancements in group III's skeletal muscle fibers is the potential correlation between vitamin D and Ator. Less hazardous metabolites may arise from vitamin D's induction of the CYP3A4 enzyme, which boosts the metabolism of several Statins, including Ator. Thus, it is proposed that taking vitamin D at the same time as Ator could lessen the possibility of its negative effects on muscle[43].

CONCLUSION

The concurrent administration of Alf prevented Ator-induced myopathy and preserved the structure of skeletal muscle fibers, as evidenced by lower CPK levels and the almost normal appearance of fibers under LM and EM. Alf can be recommended for hypercholesterolemic patients on Statins, particularly those at risk of vitamin D deficiency. It is important to ensure regular monitoring of serum calcium and vitamin D levels to prevent hypercalcemia and ensure optimal dosing of Alf.

Combining Alf with other treatments that support muscle health, such as physical therapy or antioxidants, is highly recommended due to its potential beneficial effects. Using nanoparticles to enhance the bioavailability and effectiveness of these antioxidants could be beneficial, However further research is required to minimize adverse effects and maximize their therapeutic benefits.

CONFLICTS OF INTEREST

There is no potential conflicts of interest among the authors.

REFERENCES

1. Ermakova V, Bataev H, Semenenko N. Comparative benefits of Statins in coronary heart disease. J Pharm Negative Results 2021; 12:7–13. https://doi.org/10.47750/pnr.2021.12.01.002.

2. Das KC, Hossain MU, Moniruzzaman M, Salimullah M, Akhteruzzaman S. High-Risk Polymorphisms Associated with the Molecular Function of Human HMGCR Gene Infer the Inhibition of Cholesterol Biosynthesis. Biomed Res Int. 2022; 2022:4558867. https://doi.org/10.11554558867/2022/.

3. Kow CS, Hasan SS. Meta-analysis of Effect of Statins in Patients with COVID-19. Am J Cardiol. 2020; 134:153155-. https://doi.org/10.1016/j.amjcard.2020.08.004.

4. Niedzielski M, Broncel M, Gorzelak-Pabiś P, Woźniak E. New possible pharmacological targets for Statins and ezetimibe. Biomed Pharmacother. 2020; 129:110388. https://doi.org/10.1016/j.biopha.2020.110388.

5. El-Deeb DF, Youssef MF, Yousry MM, Ahmed AM. Alfacalcidol ameliorate Atorvastatin-induced myopathy in adult male rats? A histological study. EJH. 2018; 41 (3): 11100559-. https://doi.org/10.21608/EJH.2019.25409.

6. Sultan S, Khan SU, Holden K, Hendi AA, Saeed S, Abbas A, Zaman U, Naeem S, Rehman KU. Reducing the Threshold of Primary Prevention of Cardiovascular Disease to 10% Over 10 Years: The Implications of Altered Intensity "Statin" Therapy Guidance. Curr Probl Cardiol. 2023;48(2):101486. https://doi.org/10.1016/j.cpcardiol.2022.101486.

7. Ahmed S, Saber EA, Hamouda AH, Rifaai, RA. Structural Changes in the Skeletal Muscle Fiber of Adult Male Albino Rat Following Atorvastatin Treatment; the Possible Mechanisms of Atorvastatin Induced Myotoxicity. J Cytol Histol. 2017; 8: 442. https://doi.org/10.41727099.1000442-2157/.

8. Ademi B, Folker J, Rothwell WB. Statin-induced debilitating weakness and myopathy. BMJ Case Rep. 2024 ;17(2): e256956. https://doi.org/10.1136/bcr-2023 - 256956.

9. Cipriani C, Pepe J, Piemonte S, Colangelo L, Cilli M, Minisola S. Vitamin D and its relationship with obesity and muscle. Int J Endocrinol. 2014; 2014: 841248 https://doi.org/10.1155841248/2014/.

10. Pašalić KS, Gošić K, Gavrilović A, Vojinović J. Additional impact on muscle function when treating active rheumatoid arthritis patients with high alfacalcidol doses. Vojnosanit Pregl. 2017; 74: (11)1036–1042. https://doi.org/10.2298/VSP160227300S.

11. Hou Q, Pang C, Chen Y. Association Between Vitamin D and Statin-Related Myopathy: A Meta-analysis. Am J Cardiovasc Drugs. 2022; 22(2):183-193. https://doi.org/10.1007/s402568-00492-021-.

12. Tsushima Y, Hatipoglu B. Statin Intolerance: A Review and Update. Endocr Pract. 2023 ;29(7):566-571. https://doi.org/10.1016/j.eprac.2023.03.004.

13. Khajuria DK, Disha C, Razdan R, Mahapatra DR. Efeito combinado do ácido zoledrônico e do alfacalcidol no tratamento da osteoporose por desuso em ratos [Additive effect of zoledronic acid and alfacalcidol in the treatment of disuse osteoporosis in rats]. Rev Bras Reumatol. 2015 ;55(3):24050-. Portuguese. https://doi.org/10.1016/j.rbr.2014.08.007.

14. Barclay CJ. Energy demand and supply in human skeletal muscle. J Muscle Res Cell Motil. 2017; 38(2):143155-. https://doi.org/10.1007/s10974-7-9467-017.

15. Pourghasem M, Nasiri E, Shafi H. Early renal histological changes in alloxan-induced diabetic rats. Int J Mol Cell Med. 2014; 3(1):115-. PMID: 24551816; PMCID: PMC3927393.

16. Suvarna K, Layton C, Bancroft J. Immunohistochemical techniques and Transmission electron microscopy In: Bancroft's Theory and practice of Histological Techniques, 7th ed, Churchill Livingstone Elsevier, Oxford. 2013. pp. 381426- and 492 - 538.

17. Kiernan JA. Histological and histochemical methods: Theory and practice. 5th edition. Arnold

publisher, London, New York and New Delhi; 2015;132 - 212.

18. Prats C, Gomez-Cabello A, Nordby P, Andersen JL, Helge JW, Dela F, Baba O, Ploug T. An optimized histochemical method to assess skeletal muscle glycogen and lipid stores reveals two metabolically distinct populations of type I muscle fibers. PLoS One. 2013; 8(10): e77774. https://doi.org/ 10.1371/journal.pone.0077774.

19. Emsley R, Dunn G, White IR. Mediation and moderation of treatment effects in randomised controlled trials of complex interventions. Stat Methods Med Res. 2010;19(3):23770-. https://doi.org/ 10.11770962280209105014/.

20. Kaesler N, Schreibing F, Speer T, Puente-Secades S, Rapp N, Drechsler C, Kabgani N, Kuppe C, Boor P, Jankowski V, Schurgers L, Kramann R, Floege J. Altered vitamin K biodistribution and metabolism in experimental and human chronic kidney disease. Kidney Int. 2022;101(2):338348-. https://doi.org/10.1016/j.kint.2021.10.029.

21. Banach M. Statin intolerance: time to stop letting it get in the way of treating patients. Lancet. 2022;400(10355):791793-. https://doi.org/10.1016/S01409-01643(22)6736-.

22. Caputo M, Pigni S, Agosti E, Daffara T, Ferrero A, Filigheddu N, Prodam F. Regulation of GH and GH Signaling by Nutrients. Cells. 2021;10(6):1376. https://doi.org/10.3390/cells10061376.

23. Gawish MF, Selim SA, Abd El-Star AA, Ahmed SM. Histological and immunohistochemical study of the effect of ozone versus erythropoietin on induced skeletal muscle ischemia-reperfusion injury in adult male rats. Ultrastruct Pathol. 2022 ;46(1):96109-. https://doi.org/10.108001913123.2/022.2035874.

24. Soliman ME, Atteia SE, Kefafy MA, Ali AF, Radwan EM. "Histological Study on the effect of rosuvastatin (Crestor) on the skeletal muscle of adult male albino rats and the possible protective effect of coenzyme Q10," Menoufia Medical Journal. 2017; 30 (4):1117–1124. DOI:10.4103-1110/2098.229223.

25. Southern WM, Nichenko AS, Qualls AE, Portman K, Gidon A, Beedle AM, Call JA. Mitochondrial dysfunction in skeletal muscle of fukutin-deficient mice is resistant to exercise- and 5-aminoimidazole-4-carboxamide ribonucleotide-induced rescue. Exp Physiol. 2020;105(10):17671777-. https://doi.org/10.1113/EP088812.

26. Chogtu B, Ommurugan B, Thomson SR, Kalthur SG. Effect of Vitamin D Analogue on Rosuvastatin-Induced Myopathy in Wistar Rats. Scientific World Journal. 2020; 2020:4704825. https://doi.org/10.11554704825/2020/.

27. Lindsay C, Musgaard M, Russell AJ, Sitsapesan R. Statin activation of skeletal ryanodine receptors (RyR1) is a class effect but separable from HMG-CoA reductase inhibition. Br J Pharmacol. 2022;179(21):49414957-. https://doi.org/10.1111/bph.15893.

28. Dias, C., Nylandsted, J. Plasma membrane integrity in health and disease: significance and therapeutic potential. Cell Discov, 2021; 7 (1)4. https://doi.org/10.1038/s414212-00233-020-.

29. Abdel Hamid KM, Abdel Mola AF, Meligy, FY, Abd Allah ESH. The Possible Protective Role of Ginger Extract Versus Vitamin E Against Simvastatin-Induced Skeletal Myotoxicity in Adult Male Albino Rats: Histological, Physiological and Biochemical Study. Egypt J Histol. 2017; 40, 156168-. https://doi.org/10.21608/EJH.2017.4074.

30. Sabri MH, Behare N, Alsehli AM, Berkins S, Arora A, Antoniou E, Moysiadou EI, Anantha-Krishnan S, Cosmen PD, Vikner J, Moulin TC, Ammar N, Boukhatmi H, Clemensson LE, Rask-Andersen M, Mwinyi J, Williams MJ, Fredriksson R, Schiöth HB. Statins Induce Locomotion and Muscular Phenotypes in Drosophila melanogaster That Are Reminiscent of Human Myopathy: Evidence for the Role of the Chloride Channel Inhibition in the Muscular Phenotypes. Cells. 2022 ;11(22):3528. https://doi.org/10.3390/cells11223528.

31. Ibrahim MH, Shaheen NF. Comparative study of prophylactic role of vitamin D versus coenzyme Q10 against Statin induced myopathy in adult male albino rats: Histological and Immunohistochemical study. Egypt J Histol, 2022; 71220-. https://doi.org/10.21608/EJH.2022.125297.1651.

32. Sheets K, Overbey J, Ksajikian A, Bovid K, Kenter K, Li Y. The pathophysiology and treatment of musculoskeletal fibrosis. J Cell Biochem. 2022;123(5):843851-. https://doi.org/10.1002/jcb.30217.

33. Hedberg-Oldfors C, De Ridder W, Kalev O, Böck K, Visuttijai K, Caravias G, Töpf A, Straub V,

Baets J, Oldfors A. Functional characterization of GYG1 variants in two patients with myopathy and glycogenin-1 deficiency. Neuromuscul Disord. 2019;29(12):951960-. https://doi.org/10.1016/j.nmd.2019.10.002.

34. Abdulrazaq M, Hamdan F, Al-Tameemi W. Electrophysiologic and clinico-pathologic characteristics of statin-induced muscle injury. Iran J Basic Med Sci. 2015 ;18(8):73744-. PMID: 26557961; PMCID: PMC4633455.

35. Deng JL, Zhang R, Zeng Y, Zhu YS, Wang G. Statins induce cell apoptosis through a modulation of AKT/FOXO1 pathway in prostate cancer cells. Cancer Manag Res. 2019; 11:72317242-. https://doi.org/10.2147/CMAR.S212643.

36. B Abo-Zalam H, El Denshary EED, A Abdalsalam R, A Khalil I, M Khattab M, A Hamzawy M. Revolutionizing Hyperlipidemia Treatment: Nanoencapsulated CoQ10 and Selenium Combat Simvastatin-Induced Myopathy and Insulin Resistance in Rats. Adv Pharm Bull. 2024;14(2):364-377. https://doi.org/10.34172/apb.2024.010.

37. Muraki A, Miyashita K, Mitsuishi M, Tamaki M, Tanaka K, Itoh H. Coenzyme Q10 reverses mitochondrial dysfunction in atorvastatin-treated mice and increases exercise endurance. J Appl Physiol (1985). 2012;113(3):47986-. https://doi.org/10.1152/japplphysiol.01362.2011.

38. Bouitbir J, Sanvee GM, Panajatovic MV, Singh F, Krähenbühl S. Mechanisms of statin-associated skeletal muscle-associated symptoms. Pharmacol Res. 2020; 154:104201. https://doi.org/10.1016/j.phrs.2019.03.010.

39. Dzik KP, Kaczor JJ. Mechanisms of vitamin D on skeletal muscle function: oxidative stress, energy metabolism and anabolic state. Eur J Appl Physiol. 2019 ;119(4):825839-. https://doi.org/10.1007/s0042104104--019-x.

40. Hlatky MA, Gonzalez PE, Manson JE, Buring JE, Lee IM, Cook NR, Mora S, Bubes V, Stone NJ. Statin-Associated Muscle Symptoms Among New Statin Users Randomly Assigned to Vitamin D or Placebo. JAMA Cardiol. 2023;8(1):7480-. https://doi.org/10.1001/jamacardio.2022.4250.

41. Cianferotti L, Cricelli C, Kanis JA, Nuti R, Reginster JY, Ringe JD, Rizzoli R, Brandi ML. The clinical use of vitamin D metabolites and their potential developments: a position statement from the European Society for Clinical and Economic Aspects of Osteoporosis and Osteoarthritis (ESCEO) and the International Osteoporosis Foundation (IOF). Endocrine. 2015; 50(1):12 - 26. https://doi.org/10.1007/s120200606--015-x.

42. Acevedo LM, Vidal Á, Aguilera-Tejero E, Rivero JL. Muscle plasticity is influenced by renal function and caloric intake through the FGF23-vitamin D axis. Am J Physiol Cell Physiol. 2023; 324(1):C14-C28. https://doi.org/10.1152/ajpcell.00306.2022.

43. Solomon R, Anne P, Swisher J, Nazeer B, Rosman H, Mehta RH, Maciejko JJ. Evaluating Statin Tolerability in Historically Intolerant Patients After Correcting for Subclinical Hypothyroidism and Vitamin D Insufficiency. High Blood Press Cardiovasc Prev. 2022; 29(5):409415-. https://doi.org/10.1007/s40292 - 022 - 00537 - 2.

الملخص العربي

الفاكالسيدول كعامل وقائي ضد تلف عضلة بطن الساق بعد تناول أتورفاستاتين: دراسة هستولوجية وبيوكيميائية

زينب محمد الطيب[1]، دعاء مبروك خالد[1، 2]، محمد سامي محمد[1]

قسم الهستولوجي – كلية الطب – [1]جامعة حلوان - [2]جامعة مصر للعلوم والتكنولوجيا

الخلفية والهدف: يستخدم عقار الأتورفاستاتين (أتور) على نطاق واسع لخفض نسبة الكوليسترول في الدم ولكنه غالبا ما يسبب آثارًا جانبية مرتبطة بالعضلات. أظهر ألفاكالسيدول (ألف)، وهو نظير فيتامين د، تأثيرات إيجابية على صحة العضلات .كان الهدف من العمل الحالي هو توضيح الدور الوقائي المحتمل للالفاكالسيدول علي تلف عضلة بطن الساق الناجم بعد تناول عقار الأتور في ذكور الجرذان البيضاء البالغة.

المواد والطرق: تم تقسيم 36 فأراً أبيضاً من الذكور البالغين عشوائياً إلى: المجموعة الأولى (المجموعة الضابطة)، العدد (12). المجموعة الثانية (المعالجة بعقار الأتورفاستاتين)، عدد (12)، تلقى كل فأر أتورفاستاتين (10 ميللغرام /كجم) يوميا على شكل 0.5 مل من الماء المقطر الذي يحتوي على (2) ملليغرام من أتورفاستاتين. المجموعة الثالثة (المعالجة بعقار الأتورفاستاتين والفاكالسيدول)، عدد (12)، تلقى كل فأر أتورفاستاتين كما في المجموعة الثانية بالتزامن مع الالفاكالسيدول والذي تم تعاطيه على شكل أقراص (كل 1 ميكروجرام من المادة الفعالة) تم تحضيرها عن طريق سحقها وإذابتها في 0.5 مل من الماء المقطر. تم تحضير جميع الأدوية يوميًا وإعطاؤها عن طريق الفم لمدة اربعة أسابيع. بعد اربعة وعشرين ساعة من الجرعة الأخيرة, تم التضحية بالفئران بعد تخديرهم عن طريق حقن الفينوباربيتال (80 ميللغرام/ كجم) داخل الغشاء البرتوني. تم تشريح واستئصال عينات من عضلة بطن الساق واستئصالها للدراسة النسيجية بواسطة المجهر الضوئي للصبغات التالية: (الهيماتوكسيلين والايوسين وماسون ثلاثية الألوان وصبغة PAS) بالأضافة الى اعداد بلوكات الراتين لفحصها بالمجهرالإلكتروني. كما تم إجراء دراسة بيوكيميائية لإنزيم فسفوكيناز الكرياتين (CPK). وأجريت القياسات الكمية الشكلية (المورفومترية) والدراسات الإحصائية كانت مؤكدة.

النتائج: أظهرت المجموعة الثانية تغيرات نسيجية تشير إلى الاعتلال العضلي الذي تراجع في المجموعة الثالثة. كما أشارت القيم المتوسطة لـ إنزيمات فوسفوكيناز الكرياتين(CPK) إلى زيادة ملحوظة في المجموعة الثانية مقارنة بالمجموعة الضابطة والمجموعة الثالثة. وكانت القيم المورفومترية مؤكدة.

الاستنتاجات: أثبت آلالفاكالسيدول تأثير وقائي مؤكد ضد عقار أتور في تلف العضلات الهيكلية المحدث تجريبيًا في ذكور الجرذان البيضاء. تم تأكيد هذه التأثيرات من خلال التحليلات البيوكيميائية والنسيجية ويمكن التوصية بـ آلالفاكالسيدول لمرضى ارتفاع الكوليسترول في الدم الذين يتناولون الستاتينات، وخاصة أولئك المعرضين لخطر نقص فيتامين د.

الكلمات الدالة: الالفاكالسيدول، التلف العضلي، الستاتين، التركيب الدقيق، الصبغات الخاصة.